

# Critical properties of the three-dimensional equivalent-neighbor model and crossover scaling in finite systems

Erik Luijten\*

*Department of Physics, Delft University of Technology, P.O. Box 5046, 2600 GA Delft, The Netherlands*

*Max-Planck-Institut für Polymerforschung, Postfach 3148, D-55021 Mainz, Germany*

*Institut für Physik, WA 331, Johannes Gutenberg-Universität, D-55099 Mainz, Germany<sup>†</sup>*

(November 23, 1998; corrected January 29, 1998)

Accurate numerical results are presented for the three-dimensional equivalent-neighbor model on a cubic lattice, for twelve different interaction ranges (coordination number between 18 and 250). These results allow the determination of the range dependences of the critical temperature and various critical amplitudes, which are compared to renormalization-group predictions. In addition, the analysis yields an estimate for the interaction range at which the leading corrections to scaling vanish for the spin- $\frac{1}{2}$  model and confirms earlier conclusions that the leading Wegner correction must be negative for the three-dimensional (nearest-neighbor) Ising model. By complementing these results with Monte Carlo data for systems with coordination numbers as large as 52514, the full finite-size crossover curves between classical and Ising-like behavior are obtained as a function of a generalized Ginzburg parameter. Also the crossover function for the effective magnetic exponent is determined.

64.60.Fr, 75.40.Cx, 75.10.Hk, 05.70.Fh

## I. INTRODUCTION

Over the past decades, several techniques have been applied to investigate how the critical behavior of systems depends on the range of the interactions. Before the general acceptance of the concept of universality, it was not at all clear that the critical properties of all systems with a one-component order parameter and ferromagnetic (i.e., attractive) interactions with a *finite* range are described by the Ising universality class. Since it was realized that most interactions in nature are not necessarily restricted to the nearest neighbors, one thus tried to determine the properties of models with a larger coordination number  $q$ . Another motivation, which plays a more important rôle in the present work, is the fact that in the limit of infinite interaction range one recovers the classical or mean-field model. Since the latter model can be solved analytically whereas no exact solution has been found for three-dimensional systems with a finite interaction range  $R$ , it is of interest to see how the crossover takes place from finite to infinite  $R$ . A natural choice for the examination of this crossover is the so-called “equivalent-neighbor” model, introduced by Domb and Dalton [1]. In this generalization of the Ising model, each spin interacts equally strongly with all its neighbors within a certain distance, whereas all remaining interactions are equal to zero. In Ref. [1], series expansions have been used to investigate two- and three-dimensional systems with interactions extending up to the third shell. On a simple cubic lattice this corresponds to 26 neighbors and on a face-centered cubic lattice even to 42 neighbors. While a general trend toward the mean-field properties, especially for the critical temperature, is clearly visible from these results, several problems emerge. First, with increasing interaction range, increasingly longer series are required to achieve a certain degree of convergence. Secondly, it appears that the maximum coordination numbers examined by this method are not large enough to observe the asymptotic deviations from the mean-field behavior [2]. Although Ref. [1] was published over 30 years ago, it appears that, especially in three dimensions, no substantial progress toward larger coordination numbers has been pursued. This is probably caused by the fact that also other techniques are plagued by serious difficulties upon increase of the interaction range. For example, Monte Carlo (MC) methods in general suffer from a serious decrease in efficiency if the number of interactions increases. Mon and Binder [3] studied two-dimensional (2D) spin systems with a maximum coordination number  $q = 80$ , compared to  $q = 12$  and  $q = 18$  for quadratic and triangular lattices, respectively, in Ref. [1]. Furthermore, they derived the  $R$  dependence of critical amplitudes from scaling considerations. However, it still proved difficult to reach the asymptotic regime where the predictions were expected to hold. In a subsequent paper [4], Luijten *et al.* confirmed the predictions of

---

\*Electronic address: erik.luijten@uni-mainz.de

<sup>†</sup>Present address.

Ref. [3] from a renormalization-group (RG) analysis and revealed the existence of a logarithmic  $R$  dependence in the shift of the critical temperature. Thanks to the advent of a dedicated MC algorithm for long-range interactions [5], systems with large coordination numbers could be simulated without loss of efficiency. Thus, in the same paper the critical properties were determined for quadratic systems with coordination numbers up to  $q = 436$ . It was explicitly verified that all examined systems belong to the 2D Ising universality class and the predicted  $R$  dependence of the critical amplitudes could indeed be observed, as well as the approach of the critical temperature toward its mean-field value. It is the purpose of the present work to extend this analysis to three-dimensional (3D) systems. Apart from the possibility to verify the predicted range dependences in three dimensions, a precise knowledge of the critical properties of spin models with an extended range of interaction also serves a further purpose. Namely, it allows the study of two forms of crossover in these systems. *Finite-size crossover* only pertains to finite systems at the critical temperature and denotes the transition from the classical regime where the interaction range is at least of the order of (some power of) the system size to the nonclassical (Ising) regime where the system size is much larger than the interaction range. *Thermal crossover*, on the other hand, occurs when the temperature is moved away from its critical value. The interplay between the range  $R$  of the interactions and the decreasing correlation length  $\xi$  determines the location of the crossover to classical critical behavior. If  $R$  is small, the temperature distance to the critical temperature  $T_c$  must be made rather large before  $\xi$  and  $R$  are of the same order of magnitude. In such systems, no crossover to mean-field-like critical behavior can be seen, because one has already left the critical region. However, for  $R$  large, it is well possible to observe both Ising-like and classical critical behavior. This dependence on both  $t \equiv (T - T_c)/T_c$  and  $R$  is expressed by the Ginzburg criterion [6]. Both variants of crossover have been studied for 2D systems in Refs. [7,8], which showed that accurate information on crossover scaling functions can be obtained by numerical techniques. In the light of a comparison to experimental results on the one hand and theoretical calculations of crossover scaling functions on the other hand, it is extremely relevant to investigate the 3D case as well. Here, I present the results of MC simulations of systems with interactions up to a distance of  $\sqrt{14}$  lattice units (thirteenth shell), which corresponds to 250 equivalent neighbors. Although larger interaction ranges do not diminish the efficiency of the MC algorithm, an accurate determination of the critical properties for larger  $R$  is hampered by a different effect. Indeed, such a determination is only possible in the Ising limit, which implies that the *smallest* linear system sizes must be of the order of  $L_{\min} = \mathcal{O}(R^{4/(4-d)})$  [4], where  $d$  indicates the dimensionality. Thus, for  $d = 3$  the smallest allowable systems contain of the order of  $R^{12}$  spins and one can only hope that this relation exhibits a prefactor considerably smaller than unity.

The results of the MC simulations are then used to determine the finite-size crossover functions for several quantities. It should be noted that for a full mapping of these function *very* large coordination numbers are required: simulations have been carried out for  $q$  up to 52514. Yet, an independent determination of the critical temperature of these systems is not required, but can be obtained by extrapolation. It suffices thus to study modest ( $L \leq 40$ ) system sizes for these interaction ranges. The determination of thermal crossover functions will be the subject of a future paper [9], as it requires calculations which are actually complementary to those of the present work (results for the susceptibility can be found in Ref. [10]). Indeed, for a determination of the critical properties by finite-size scaling and for the mapping of the finite-size crossover functions, all data must lie within the finite-size regime, whereas for thermal crossover scaling care must be taken that the data lie outside this regime.

Two further questions that are addressed in this paper concern the corrections to scaling. In the first place, the range dependence of the thermal finite-size corrections is shown to be in very good agreement with the predictions of Ref. [4]. Secondly, the finite-size corrections due to the leading irrelevant field are analyzed and the related variation of the  $\phi^4$  coefficient in the Landau-Ginzburg-Wilson (LGW) Hamiltonian is obtained. This permits an estimation of the interaction range for which this coefficient coincides with its fixed-point value and confirms that for the three-dimensional nearest-neighbor Ising model it does not lie between the Gaussian fixed point and the Ising fixed point.

The outline of this paper is as follows. In Sec. II, I briefly summarize earlier predictions for the range dependence of critical amplitudes and discuss the shift of the critical temperature as a function of interaction range. Section III gives details of the Monte Carlo simulations. Furthermore, the determination of the critical temperatures is discussed as well as the analysis of the range dependence of corrections to scaling. The variation of critical amplitudes as a function of interaction range is treated in Sec. IV and finite-size crossover curves are obtained in Sec. V. I end with some concluding remarks in Sec. VI.

## II. SUMMARY OF RENORMALIZATION-GROUP PREDICTIONS

In the absence of an external field, the equivalent-neighbor or medium-range model is defined by the following Hamiltonian,

$$\mathcal{H}/k_B T = - \sum_{\langle ij \rangle} K(\mathbf{r}_i - \mathbf{r}_j) s_i s_j, \quad (1)$$

where  $s = \pm 1$ , the sum runs over all spin pairs and the spin-spin coupling is defined as  $K(\mathbf{r}) = J > 0$  for  $|\mathbf{r}| \leq R_m$  and  $K(\mathbf{r}) = 0$  for  $|\mathbf{r}| > R_m$ . I first summarize the findings of Ref. [4] for the  $R$  dependence of critical properties, as obtained by an RG analysis. Although at first sight this approach is not very different from a simple scaling analysis, it offers several advantages. The formulation in terms of two competing fixed points provides a clear insight into the crossover mechanism: for  $R$  large the coefficient of the  $\phi^4$  term in the LGW Hamiltonian is suppressed with respect to the quadratic term in this expression. Thus, the renormalization trajectory passes close to the Gaussian fixed point and the critical amplitudes pick up a specific  $R$  dependence which is determined by the flow near this fixed point. For any finite  $R$ , the system will still flow to the neighborhood of the nontrivial (Ising) fixed point (cf. Fig. 1 in Ref. [4]). However, the  $R$  dependence reveals some aspects of the Gaussian fixed point which are not normally seen in Ising-like systems. For example, near this fixed point the thermal exponent  $y_t$  and the leading irrelevant exponent  $y_i$  assume the values 2 and  $4 - d$ , respectively, which coincide for  $d = 2$ . Such a coincidence would lead to logarithmic factors in the scaling functions, were it not that the Gaussian fixed point is unstable for  $d = 2$ . In contrast, the  $R$  dependence of scaling functions indeed allows the observation of such logarithms. The occurrence of these dependences is not easily found from a scaling analysis.

For the magnetization density  $m$  and the magnetic susceptibility  $\chi$  the following range dependences have been obtained,

$$m \propto t^\beta R^{(2d\beta-d)/(4-d)}, \quad (2)$$

$$\chi \propto t^{-\gamma} R^{2d(1-\gamma)/(4-d)}, \quad (3)$$

where  $\beta$  and  $\gamma$  denote the standard Ising critical exponents. Furthermore, the finite-size scaling behavior of these quantities was derived as

$$m = L^{y_h-d} R^{(3d-4y_h)/(4-d)} \hat{f}_s^{(1)} \left( t L^{y_t} R^{-2(2y_t-d)/(4-d)}, \tilde{u} L^{y_i} R^{-4y_i/(4-d)}, h L^{y_h} R^{(3d-4y_h)/(4-d)} \right), \quad (4)$$

$$\chi = L^{2y_h-d} R^{2(3d-4y_h)/(4-d)} \hat{f}_s^{(2)} \left( t L^{y_t} R^{-2(2y_t-d)/(4-d)}, \tilde{u} L^{y_i} R^{-4y_i/(4-d)}, h L^{y_h} R^{(3d-4y_h)/(4-d)} \right). \quad (5)$$

Here,  $\hat{f}_s^{(i)}$  denote universal scaling functions,  $y_t$  and  $y_i$  are the thermal and leading irrelevant exponent introduced before, and  $y_h$  is the magnetic exponent.  $\tilde{u}$  and  $h$  are the irrelevant and the magnetic scaling field, respectively.

Also the shift of the critical temperature with respect to its mean-field value has been calculated in Ref. [4]. However, this treatment left several questions unanswered, which I will consider here in some more detail. A clear understanding of the nature of this shift is of particular significance for the crossover scaling, since one has to calculate the critical temperatures for systems with large coordination numbers by means of extrapolation. It was derived that under a renormalization transformation the contribution of the  $\phi^4$  term to the quadratic term in the LGW Hamiltonian leads to a range-dependent shift of the reduced temperature  $t \equiv (T - T_c)/T_c$ . For  $d = 2$  it was found in Ref. [4] that this shift has the form

$$T_c - T_c^{\text{MF}} = \frac{c_0 + c_1 \ln R}{R^2} + \dots \quad (6)$$

where  $c_0$  and  $c_1$  are constants. This expression has also been confirmed numerically, see Fig. 4 in Ref. [4]. Interestingly, this result has been recovered in Ref. [11], where in addition it was found that the constant  $c_1$  has a universal value  $-2/\pi \approx -0.6366$ . Indeed, this agrees with the value  $-0.624$  (7) obtained from an analysis of the available data for  $25 \lesssim R^2 \lesssim 70$ . (The somewhat lower value 0.609, corresponding to the coefficients quoted in Ref. [8], can be explained from the influence of the data point at  $R^2 = 16.2$ .) However, the result for general  $2 < d < 4$ , a shift proportional  $R^{-2d/(4-d)}$ , clearly contradicts the results obtained from systematic expansions in terms of the inverse coordination number (but see the remarks at the end of this section). Brout [12] obtained to leading order a shift of the form  $1/q \propto 1/R^d$ . This result was recovered by Vaks *et al.* [13] and Dalton and Domb [14]. As indicated in Ref. [15], such an additional and actually dominant shift can also be obtained from the RG analysis by allowing for a (spherically symmetric) lower-distance cutoff  $a$  in the spin-spin coupling  $K(\mathbf{r})$ . In momentum space the coupling then takes the form

$$\tilde{K}(\mathbf{k}) = c \left( \frac{2\pi}{kR} \right)^{d/2} J_{d/2}(kR) - c \left( \frac{a}{R} \right)^d \left( \frac{2\pi}{ka} \right)^{d/2} J_{d/2}(ka), \quad (7)$$

where  $c = JR^d$  and  $J_\nu$  is a Bessel function of the first kind of order  $\nu$  (cf. Eq. (A3) in Ref. [4]). The second term in this expression yields an additional contribution to the quadratic term in the LGW Hamiltonian, which is

precisely the  $1/R^d$  shift obtained by Brout. Furthermore, it contributes to the  $k$ -dependent part of this term, which via the rescaling of the field (see Ref. [4]) leads to a  $1/R^{d+2}$  shift. Note that, upon expansion in powers of  $R$ , a formulation in terms of the coordination number  $q$  implies such a shift as well. At even higher order, one finds (at rational dimensionalities) additional  $\ln R$  dependences, as was first recognized by Thouless [2].<sup>1</sup> He has studied a modified form of the Ising model, where the system is divided into cells within which the spin-spin interactions are constant. The shift of the critical temperature as a function of the cell size is then calculated by means of perturbation theory. In three dimensions, the leading-order result of Brout is recovered, namely a shift proportional to  $1/q$ . In the next-to-leading term a logarithmic dependence on the coordination number is obtained,

$$T_c - T_c^{\text{MF}} = \frac{a_1}{q} + a_2 \frac{\ln q}{q^2} + \dots, \quad (8)$$

whereas for  $d = 2$  the logarithm emerges already in the leading term,

$$T_c - T_c^{\text{MF}} = b_1 \frac{\ln q}{q} + \dots. \quad (9)$$

The latter expression is in perfect agreement with Eq. (6), whereas the logarithm in the higher-order term in (8) has not been found in Refs. [4,15]. Since the logarithms in Eqs. (8) and (9) apparently follow from the same mechanism and the factor  $\ln R$  in Eq. (6) is specific for the two-dimensional case (where all higher-order terms in the LGW Hamiltonian are equally relevant), I conclude that there must be two different sources for the logarithms, which happen to yield the same effect in  $d = 2$ . Indeed, the logarithms in Eqs. (8) and (9) arise from counter terms canceling the infrared divergences in the perturbation expansion. This appears to be intimately linked to the infrared divergences occurring in massless super-renormalizable field theories at rational dimensionalities [16]. Actually, the treatment of Ref. [4] *does* account for logarithmic factors in  $d = 3$ , although at much higher order. For systems with a large interaction range, the first part of the renormalization trajectory passes close to the Gaussian fixed point. Near this fixed point, only the  $\phi^4$  term is relevant for  $d = 3$  and all terms  $\phi^n$  with  $n > 6$  are irrelevant. The marginal character of the  $\phi^6$  term produces a logarithmic range dependence in the shift of the critical temperature. However, since this logarithm stems from the term quadratic in  $\phi^6$  and the field  $\phi$  is rescaled by a factor  $R^{-1}$ , this contribution is extremely weak. An actual calculation shows that it leads to a shift proportional to  $\ln R/R^{18} \propto \ln q/q^6$ . In addition, the  $\phi^6$  term will yield a correction of order  $R^{-8}$ . However, it may be added that it is generally expected [17] that such high composite operators have very little influence near the Ising fixed point.

Let me now briefly return to the leading shift  $R^{-2d/(4-d)}$  obtained in Ref. [4]. It is instructive to note that this shift is consistent with crossover arguments first given by Riedel and Wegner [18]. Indeed, the Ginzburg criterion states that a crossover from classical to nonclassical critical behavior occurs as a function of the crossover parameter  $t^{(4-d)/2}R^d$ . In terms of a more general formulation, this parameter is written as  $t^\phi/g$ , with  $\phi = (4-d)/2$  and  $g = R^{-d}$ . The crossover exponent  $\phi$  (not to be confused with the field  $\phi$ ), introduced in Ref. [18], is just the exponent  $4-d$  of the relevant operator driving the system away from the Gaussian fixed point (i.e., the  $\phi^4$  term in the LGW Hamiltonian), divided by the thermal exponent  $y_t = 2$ . Then, on general grounds [18,19], the shift of  $T_c$  is predicted to scale as  $g^{1/\phi} \propto R^{-2d/(4-d)}$ . This is another indication that the shift terms in Eq. (8) originate from a different, complementary mechanism. In addition, it is noted that the formulation in terms of the crossover exponent  $\phi$  can be carried even further (see, e.g., Ref. [20]). Indeed, for any thermodynamic quantity  $P$  which is near the Ising critical point proportional to  $t^{x_1}$ , the combined dependence on  $g$  and  $t$  will be

$$P \propto g^{(x_G - x_1)/\phi} t^{x_1}, \quad (10)$$

where  $x_G$  denotes the  $t$  dependence of  $P$  near the Gaussian fixed point. In terms of  $t$  and  $R$ , this can be written as

$$P \propto R^{d(x_1 - x_G)/\phi} t^{x_1}, \quad (11)$$

which yields, e.g.,  $m \propto R^{2d(\beta-1/2)/(4-d)} t^\beta$  and  $\chi \propto R^{2d(1-\gamma)/(4-d)} t^{-\gamma}$ , recovering Eqs. (2) and (3).

### III. MONTE CARLO SIMULATIONS

---

<sup>1</sup>This work only came to the attention of the author after the publication of Ref. [4].

## A. Simulational details

I have carried out extensive simulations of 3D simple cubic lattices consisting of  $L \times L \times L$  lattice sites with periodic boundary conditions. Each spins interacts equally with its  $q$  neighbors lying within a distance  $R_m$ , i.e., the system is described by the Hamiltonian (1). For the simulations I have used the cluster MC algorithm introduced in Ref. [5]. Its application to the present case is described in more detail in the appendix of Ref. [4]. In order to avoid lattice effects I formulate the analysis in terms of an effective interaction range  $R$  [3],

$$R^2 \equiv \frac{\sum_{j \neq i} (\mathbf{r}_i - \mathbf{r}_j)^2 K_{ij}}{\sum_{j \neq i} K_{ij}} = \frac{1}{q} \sum_{j \neq i} |\mathbf{r}_i - \mathbf{r}_j|^2 \quad \text{with } |\mathbf{r}_i - \mathbf{r}_j| \leq R_m. \quad (12)$$

It is easily seen that  $\lim_{R \rightarrow \infty} R^2 = 3R_m^2/5$ . Table I lists  $R_m$ ,  $q$ , and  $R$  for the first thirteen neighbor shells which have been examined in the present work.

Several tests have been carried out to check the implementation of the algorithm. For  $R_m^2 = 1$  exact results (for  $L = 3, 4$ ) and accurate MC data are given in Ref. [21] and for  $R_m^2 = 2, 3$  alternative MC programs were available, allowing the verification of the data for various system sizes. I have carried out very long Monte Carlo simulations ( $10^9$  and  $10^8$  Wolff clusters, respectively) for  $L = 4$  and  $L = 20$  for these ranges, at couplings close to  $K_c(R)$ . On the other hand, if one takes into account all lattice symmetries, an explicit summation over all states is feasible for  $L = 3$  ( $2^{27} \approx 1.34 \times 10^8$  configurations). For this case, I have carried out simulations for all ranges  $1 \leq R_m^2 \leq 14$ . No systematic deviations could be observed. The actual simulations were carried out for systems up to  $L = 200$  (8 million spins); the number of samples was chosen depending on the system size. As a rule of thumb, the amplitude ratio  $Q$  (to be defined below) had a relative accuracy on the permille level for the largest systems.

## B. Determination of the critical temperatures

In order to analyze the range dependence of several quantities, an accurate knowledge of the critical temperature for each single value of  $R_m$  is required. The critical temperatures of systems with interaction ranges corresponding to the first thirteen neighbor shells have been determined using the amplitude ratio  $Q_L = \langle m^2 \rangle_L^2 / \langle m^4 \rangle_L$ . For the 3D Ising universality class and a cubic geometry with periodic boundary conditions, this quantity has, in the thermodynamic limit, the universal critical-point value  $Q = Q_I = 0.6233$  (4) [21]. As mentioned in Sec. I, an accurate determination of the critical point is mainly hampered by the requirement that one must reach the Ising limit, i.e.,  $L_{\min} \approx R^4$ . For the inner shells, the smallest system sizes that could be used in the finite-size analysis were of the same order as in an analysis of the 3D nearest-neighbor Ising model, i.e.,  $L \gtrsim 5$ . For the remaining shells, the smallest allowable system sizes, as determined from the quality of the least-squares fits, followed the restriction  $L \gtrsim R^4$  rather closely. Only for the outermost shells this criterion could be slightly relaxed. Thus, the accuracy of the fit results decreases considerably with increasing interaction range, because the finite-size data cover a much smaller range of system sizes and all the accurate results for small system sizes have to be excluded from the analysis. The least-squares fits were made using the finite-size expansion for  $Q$  given in Ref. [21],

$$Q_L(K) = Q + a_1(K - K_c)L^{y_t} + a_2(K - K_c)^2 L^{2y_t} + \dots + b_1 L^{y_i} + b_2 L^{2y_i} + \dots, \quad (13)$$

where  $K$  denotes the spin-spin coupling,  $K_c$  the critical coupling, and the  $a_i$  and  $b_i$  are nonuniversal (range-dependent) coefficients. The exponents  $y_t$  and  $y_i$  are the thermal and leading irrelevant exponent, respectively. They are approximately given by:  $y_t = 1.587$  (2) and  $y_i = -0.82$  (6) [21], where the latter exponent was kept fixed in all analyses. Table II shows my resulting estimates for  $Q$  and  $K_c$ . In the first place, one notes that all systems belong, within the statistical accuracy, to the 3D Ising universality class. The critical couplings for the first three shells are in agreement with the old series-expansion results of Domb and Dalton. In order to improve the accuracy of the results, I have repeated all analyses with  $Q$  fixed.

The results of the finite-size analyses permit some additional tests of the scaling predictions of Refs. [3,4]. Indeed, the range dependence of the thermal coefficient  $a_1$  in Eq. (13) should take the same form as the first argument of the universal scaling functions (4) and (5). Upon expansion of such a scaling function one finds a temperature-dependent argument of the form  $aL^{y_t} R^{-2(2y_t-d)/(4-d)} \approx -a[(K - K_c)/K_c]L^{y_t} R^{-2(2y_t-d)/(4-d)}$ , where  $a$  is a constant that does not depend on  $R$ . Thus  $a_1 = -aR^{-2(2y_t-d)/(4-d)}/K_c \sim R^{-2(2y_t-d)/(4-d)} \times R^d \sim R^{2.652} \sim q^{0.884}$ . Figure 1 shows  $a_1$  as a function of the coordination number  $q$ . Both a curve  $\sim q^{0.884}$  and a reference line with slope 1 are shown; evidently

the former describes the numerical data very well. Deviations for relatively small  $q$  are not disturbing, since the RG predictions are only valid in the limit of large interaction ranges and the small- $q$  data may also exhibit some lattice effects.

Of particular interest is also the range-dependence of the coefficient  $b_1$  in Eq. (13), because this coefficient is proportional to  $(u - u^*)/u^*$ , where  $u$  is the coefficient of the  $\phi^4$  term in the LGW Hamiltonian and  $u^*$  is its fixed-point value [22]. As such,  $b_1$  yields information on the  $R$  dependence of the size and sign of the corrections to scaling that appear in the Wegner expansion [23]. This expansion describes the singular corrections to the asymptotic temperature dependence of thermodynamic quantities close to the critical point. For example, if  $u/u^* > 1$  the leading coefficient in the expansion for the susceptibility will have a negative sign and hence the susceptibility exponent  $\gamma$  will approach the Ising value from *above*, cf. also Ref. [24]. On the other hand, if  $u$  lies between the Gaussian and the Ising fixed point, i.e.,  $0 < u/u^* < 1$ , the sign of the first Wegner correction will be positive and  $\gamma$  will approach the Ising value from below. In order to extract the  $R$  dependence of  $u$  from the coefficient  $b_1$ , the RG scenario of Ref. [4] has to be reconsidered. It can be shown that in the large- $R$  limit  $u = u_0/R^4$ . Because  $u_0$  will exhibit a remaining, weak  $R$  dependence for small  $R$ , I write it as  $u_0(R)$ . The first part of the RG transformation is just a scale transformation in the neighborhood of the Gaussian fixed point, which cancels the factor  $1/R^4$  in  $u$ . The  $\phi^4$  coefficient can now be written as  $u_0(R) = u^* + [u_0(R) - u^*]$ , which close to the Ising fixed point scales as  $u_0 \rightarrow u'_0 = u^* + [u_0(R) - u^*]L^{y_i}R^{-4y_i/(4-d)}$  [4]. Thus, the coefficient  $b_1$  in Eq. (4) is equal to  $c[\bar{u}(R) - 1]R^{-4y_i/(4-d)}$ , where  $\bar{u}(R) \equiv u_0(R)/u^*$  and  $c$  is a nonuniversal proportionality constant. For  $R$  large,  $\bar{u}(R)$  should go to a finite constant and hence  $b_1$  is expected to be proportional to  $R^{-4y_i/(4-d)}$  in this limit. Just as for most other quantities, it is difficult to accurately determine  $b_1$  for large interaction ranges, because the small system sizes have to be omitted from the analysis. Nevertheless, the results shown in Fig. 2 appear to be well compatible with the predicted  $R$  dependence, with  $c[\bar{u}(\infty) - 1] \approx -0.14$  (the latter estimate relies on the assumption that the asymptotic limit has actually been reached for the largest ranges shown in the figure). Unfortunately, no estimate for  $u_0(R)$  for either  $R = 1$  (nearest-neighbor Ising model) or any other  $R$  is known to the author, so that the overall constant  $c$  [which would have permitted the calculation of  $u_0(R)$  from  $b_1(R)$ ] cannot be determined (cf. also Ref. [25]).

On the other hand, an estimate of the interaction range where  $\bar{u}(R) = 1$  does not depend on  $c$ , and so it can be predicted with a reasonable accuracy that this condition is fulfilled at  $R^2 \approx 1.56$ . The interest of this point lies in the fact that the leading corrections to scaling should vanish there, which in principle allows a much more accurate determination of critical properties from numerical simulations. This approach was used for the first time in Ref. [21], where, amongst others, a spin- $\frac{1}{2}$  model with nearest-neighbor coupling  $K_{nn}$  and third-neighbor coupling  $K_{3n}$  was simulated. The ratio  $K_{3n}/K_{nn}$  was set to 0.4, which in hindsight proved to be somewhat too strong for fully suppressing the leading corrections to scaling. A newer estimate yielded  $K_{3n}/K_{nn} = 0.25$  (2) as an optimal choice [26]. Further studies of these systems were presented in Ref. [27], where the coupling constant ratio was systematically varied in order to eliminate the leading finite-size corrections. This led to an estimate of  $K_{3n}/K_{nn} \approx 0.27$ . Both estimates turn out to be in quite good agreement with my prediction for *general* interaction profiles. Indeed, as follows from Eq. (12), an effective interaction range  $R^2 = 1.56$  can be obtained by, e.g., nearest-neighbor and next-nearest neighbor interactions with  $K_{2n}/K_{nn} = 0.64$  or by nearest and third-neighbor interactions with  $K_{3n}/K_{nn} = 0.29$ . This also explains the finding of Ref. [21] that  $K_{2n}$  had to be chosen much larger than  $K_{3n}$  to reach the same effect.

In this context it is of interest to review some series-expansion results for the leading correction amplitudes for the magnetization, the susceptibility, and the correlation length on simple cubic (sc), body-centered cubic (bcc), and face-centered cubic (fcc) lattices. Liu and Fisher [22] concluded that the leading correction amplitudes are *negative* for the sc and bcc lattices and gave various arguments that this also holds for the fcc lattice. Furthermore, they argue that these amplitudes should vanish monotonically with coordination number ( $q = 6, 8, 12$ , respectively). This is indeed confirmed by the fact that the data in Fig. 2 *monotonically* approach the predicted asymptotic  $R$  dependence, apart from statistical scatter. However, from the fact that for the sc lattice with  $q = 18$  ( $R^2 = 5/3$ ) the finite-size corrections have already changed sign, it would be expected that the correction amplitudes for the fcc lattice are close to zero. In contrast, both the results of George and Rehr [28] and Liu and Fisher [29], see Table III, exhibit a relatively weak variation with coordination number. On the basis of these results one would certainly expect the leading corrections to vanish at much higher coordination numbers. Thus, I conclude that, apart from the dependence on  $q$  (or  $R$ ), the value of  $u$  has a rather strong dependence on the lattice structure as well. For completeness, it may be remarked that the analyses of the Monte Carlo data for the magnetization density and the susceptibility have revealed the same monotonic  $R$  dependence of the leading correction amplitude as that of the quantity  $b_1$  discussed above.

#### IV. RANGE DEPENDENCE AT CRITICALITY

## A. Critical temperature

The estimates for the critical coupling as given in Table II can in principle be used to verify the predictions for the shift of the critical temperature. Because lattice effects are still relatively strong for the interaction ranges studied here, the coordination number  $q$ , appearing in, e.g., Eq. (8), cannot be used directly. It is expected that these lattice effects disappear when the *effective* interaction range  $R$  is used instead. Thus, the predicted shift is rewritten as:

$$T_c^{-1} \equiv qK_c = 1 + \frac{c_0}{R^3} + \frac{c_1}{R^5} + \frac{c_2 + c_3 \ln R}{R^6} + \dots, \quad (14)$$

where I have used the inverse critical temperature to conform to the earlier literature. Unfortunately, it turns out that even in terms of  $R$  the numerical data exhibit remarkably strong scatter for  $R_m^2 \leq 10$ , making it impossible to obtain a sensible fit for the smaller interaction ranges. On the other hand, for  $R_m^2 > 10$ , Eq. (14) describes the data very well. Because of the small variation of the  $\ln R$  term over the fit range, it was not possible to discern the coefficients  $c_2$  and  $c_3$ . Thus, I have omitted  $c_2$  altogether, which implies that this coefficient is absorbed into an effective value of  $c_3$ . The resulting fit yielded the values  $c_0 = 0.498$  (2),  $c_1 = -5.7$  (7), and  $c_3 = 7.1$  (9). Clearly, the last two estimates suffer from the fact that (for the available values of  $R$ ) the last two terms in Eq. (14) lie quite close. Thus, it cannot be excluded that the high values of  $c_1$  and  $c_3$  are partially caused by a mutual cancellation and that apart from the quoted statistical errors there is a considerable systematic error. Nevertheless, as will be seen below, the accuracy of the resulting expression is sufficient to obtain rather precise estimates for systems with larger interaction ranges. In fact, if the results for  $R_m^2 = 9, 10$  are also included in the least-squares fit and the lattice effects are simply ignored, an essentially phenomenological interpolation formula is obtained, which for larger ranges turns out to agree very well with the first fit.

In Refs. [14,2], series-expansion estimates are given for the coefficients  $c_0$  and  $c_3$  in (14). In terms of an expansion in  $q$ , Dalton and Domb found the value 4.46 for the leading coefficient (confusingly, in later work [1,30] the value 3.5 was quoted) and for the prefactor of the logarithm Thouless obtained  $-2000/27 \approx -74.1$ . To compare these values to  $c_0$  and  $c_3$ , I write  $q + 1 \approx \frac{4}{3}\pi R_m^3 \approx \frac{4}{3}\pi(\frac{5}{3})^{3/2}R^3 \approx 9.013R^3$ . This yields  $c_0 = 0.495$  and  $c_3 = -2.74$ . In view of the various approximations that have been made, the agreement for  $c_0$  is truly remarkable. Because of the above-mentioned cancellation effects and because of the omission of  $c_2$  in the fit, a sensible comparison for  $c_3$  is not possible. However, we note that also Thouless finds a relatively high value for  $c_3$ . Figure 3 shows the various predictions for the shift of the inverse critical temperature.

## B. Magnetization density

In the Monte Carlo simulations, I have sampled the absolute magnetization density  $\langle |m| \rangle$ . The dependence of this quantity on both  $L$  and  $R$  is given by Eq. (4), from which the following finite-size expansion can be derived,

$$m_L(K, R) = L^{y_h-d} \{ d_0(R) + d_1(R)[K - K_c(R)]L^{y_t} + d_2(R)[K - K_c(R)]^2 L^{2y_t} + \dots + e_1(R)L^{y_i} + \dots \}. \quad (15)$$

For each single value of  $R$ , I have fitted the numerical data to this expression. The critical couplings obtained from this analysis are in agreement with those shown in Table II. The corresponding estimates for  $y_h$  are listed in Table IV. The slight tendency of the estimates to decrease with increasing  $R$ , as well as the increasing uncertainties, can be explained from the requirement that the smallest system size included in the analysis must increase with  $R$ . When the analyses were repeated with the critical couplings fixed at the best values in Table II, the agreement of the estimates for  $y_h$  (also shown in Table IV) with the 3D Ising value  $y_h = 2.4815$  (15) [21] was even better. Thus, this confirms the expectation that all these systems belong to the Ising universality class. The critical amplitudes  $d_0(R)$  can be used to extract the leading range dependence of the magnetization density. In order to maximize the accuracy in these amplitudes, the results shown in Table IV were obtained with the exponents  $y_h$  and  $y_t$  fixed at their Ising values (but the critical coupling  $K_c$  was included as a free parameter). A fit of  $d_0(R)$  to the form  $d_0(R) = dR^x$  for the largest three values of  $R$  yielded  $x = -0.87$  (5), somewhat (although not significantly) smaller than the predicted value  $x = (3d - 4y_h)/(4 - d) = -0.926$  (6). This shows that the asymptotic regime, where higher-order corrections can be neglected, has not yet been reached. In general, the corrections are powers of  $R^{-2}$  [4]:

$$d_0(R) = dR^x \left( 1 + \frac{A_1}{R^2} + \frac{A_2}{R^4} + \dots \right) \quad (16)$$

Expression (16) with one correction term allowed me to obtain a very acceptable fit ( $\chi^2/\text{DOF} \approx 0.6$ ) for *all* data points with  $2 \leq R_m^2 \leq 14$  and yielded  $x = 0.923$  (5), in excellent agreement with the RG prediction of Ref. [4]. Figure 4 shows the MC results for  $d_0(R)$  together with the asymptotic range dependence and the full fit to the renormalization expression.

### C. Susceptibility

At criticality, the magnetic susceptibility is directly proportional to the average square magnetization. Thus, I have fitted the Monte Carlo data, for each interaction range separately, to an expression of the form

$$\chi_L(K, R) = s_0 + L^{2y_h - d} \{ p_0(R) + p_1(R)[K - K_c(R)]L^{y_t} + p_2(R)[K - K_c(R)]^2 L^{2y_t} + \dots + q_1(R)L^{y_t} + \dots \}, \quad (17)$$

where the additive constant  $s_0$  originates from the analytic part of the free energy. In the further analysis, this constant has been set to zero, because it tends to interfere with the leading irrelevant term  $q_1(R)L^{y_t}$ . Just as for the absolute magnetization density, I list estimates for the magnetic exponent  $y_h$  (Table V). Although, as expected, the uncertainty increases with  $R$ , one observes that all estimates agree with the Ising value. Also the critical couplings agree with those obtained from the fourth-order amplitude ratio and  $\langle |m| \rangle$ . Thus, I have repeated all analyses with  $K_c$  fixed; the corresponding results for  $y_h$  are shown in Table V as well. Finally, I have fixed the magnetic exponent at  $y_h = 2.4815$  (but included  $K_c$  as a free parameter) in order to obtain accurate estimates for  $p_0(R)$  (Table V). Fitting a straight line  $pR^{-x}$  to the last three values yielded a slope  $-1.73$  (9), which is consistent with the prediction  $-1.852$  [Eq. (5)]. A fit formula with one additional correction term,  $pR^{-x}(1 + bR^{-2})$ , allowed the inclusion of several more data points and yielded  $x = -1.92$  (11). Both fits and the numerical data are shown in Fig. 5.

### D. Connected susceptibility

In principle, the *connected* susceptibility, given by

$$\tilde{\chi} = L^d \frac{\langle m^2 \rangle - \langle |m| \rangle^2}{k_B T}, \quad (18)$$

can be treated in the same way as the absolute magnetization density and the susceptibility. The main drawback of this quantity, being the difference of two fluctuating quantities, is that its statistical accuracy is relatively poor. Nevertheless, the magnetic exponents extracted from the numerical data for the individual interaction ranges are consistent with the Ising value and the finite-size amplitudes can be used to determine the range dependence of the connected susceptibility. As shown in Ref. [8], knowledge of this dependence is very useful to determine the thermal crossover curve for the susceptibility (which for  $T < T_c$  is represented by  $\tilde{\chi}$ ) from data for different  $R$ , because it makes it possible to divide out the subleading range dependence of this curve. Rather than giving the full details of the analysis, I restrict myself to Fig. 6, which shows the critical amplitudes together with the RG prediction fitted to it. Instead of  $\tilde{\chi}$ , the so-called scaled susceptibility  $k_B T \tilde{\chi}$  is often considered. It has been noted for the two-dimensional case [8], that the latter quantity exhibits considerably stronger deviations from the asymptotic range dependence, which are caused by the shift of the critical temperature. Figure 6 confirms that this also holds for the three-dimensional case.

## V. FINITE-SIZE CROSSOVER

### A. General considerations

As stated in the introduction, the critical properties of the equivalent-neighbor models obtained in the previous section can now be used to find the finite-size crossover scaling functions describing the crossover from a finite mean-field-like system to a finite Ising-like system at  $T = T_c$ . A detailed description of this phenomenon has been given in Ref. [8]. Qualitatively this crossover can simply be understood from the observation that systems with a linear size of the order of the interaction range are essentially mean-field-like systems, which are turned into systems with a short-range interaction if the system size grows beyond the interaction range. RG considerations have shown that the crossover is ruled by a generalized Ginzburg parameter  $G \equiv LR^{-4/(4-d)}$ , so that the mean-field regime corresponds to  $G \ll 1$  and the Ising regime to  $G \gg 1$ . The expression for  $G$  has also been obtained in Ref. [31]. It is numerically not feasible to observe the entire crossover regime in a system with fixed  $R$  by merely varying the system size, since it spans several decades in the parameter  $G$ . Thus, I construct the crossover curve by combining the results for various interaction ranges, just as this has been done for the two-dimensional case in Ref. [8] and for the three-dimensional thermal crossover in Ref. [10]. Since it turns out that for  $L \lesssim 20$  the curves are affected by nonlinear finite-size effects, the smallest value of the crossover parameter that can be reached with the interaction ranges studied in the previous two sections is  $20/(9.168)^2 \approx 0.24$ . The true mean-field regime, however, is only reached



for *much* smaller  $G = \mathcal{O}(10^{-4})$ . Thus, I have carried out simulations for systems with effective interaction ranges up to  $R^2 = 323.81$  ( $R_m^2 = 540$ ), corresponding to coordination numbers as large as  $q = 52514$ . Evidently, the Monte Carlo algorithm introduced in Ref. [5] comes to its full glory here: The simulation of three-dimensional systems with so many interactions present would not have been feasible with either a Metropolis-type algorithm or a conventional cluster-building algorithm. The actual crossover curves shown below are obtained from a combination of the data for  $2 \leq R_m^2 \leq 14$ , with system sizes between  $L = 20$  and  $L = 200$ , and additional data for 20 different interaction ranges  $18 \leq R_m^2 \leq 540$ . For the latter systems, the critical coupling was determined using the extrapolation formula discussed in Sec. IV A and subsequently simulations were carried out for  $20 \leq L \leq 40$  at each single value of  $R_m^2$ .

An additional complication is formed by the regime  $G \gg 1$ . Whereas this part of the crossover curve can easily be reached by simulating large system sizes with very small interaction ranges, higher-order range dependences prevent the direct use of these data for the construction of crossover curves. It was recognized in Ref. [8] that these are the same corrections that are responsible for the deviations from the asymptotic range dependence in Figs. 4, 5, and 6, so that this effect can be removed by dividing the magnetization density by the factor in brackets in Eq. (16) and the other quantities by the corresponding counterparts of this factor.

## B. Magnetization density

As follows from Eq. (4), the magnetization density  $\langle |m| \rangle$  at criticality is proportional to  $L^{y_h - 3}$  in the Ising regime. The prefactor depends on the interaction range and scales as  $R^{9 - 4y_h}$ . On the other hand,  $\langle |m| \rangle$  is independent of  $R$  in the mean-field regime and just scales as  $N^{-1/4} \propto L^{-3/4}$ . If the crossover behavior can indeed be described in terms of a single variable  $G = L/R^4$ , a data collapse should be obtained for  $\langle |m| \rangle L^{3/4}$ . In the mean-field regime, this quantity is independent of  $G$  and in the Ising regime it scales as  $G^{y_h - 9/4}$ . The resulting curve for this quantity is shown in Fig. 7. It is immediately clear that the data lie on a perfectly smooth curve, confirming that the crossover is indeed ruled by the generalized Ginzburg parameter  $G$ . The correction parameter  $C[m] = 1 + A_1 R^{-2}$  refers to the higher-order range dependences which have been divided out, in order to make the data for small  $R$  collapse on the same (Ising) asymptote. For large interaction ranges this correction factor rapidly approaches unity. In the graph I have included a line with slope  $y_h - 9/4 = 0.2315$ , indicating the dependence on  $G$  in the Ising regime. Whereas no exact result exists for the finite-size amplitude of this asymptote, it is possible to calculate its counterpart in the mean-field regime, where it is found that [8]

$$\langle |m| \rangle L^{3/4} = 12^{1/4} \frac{\Gamma(\frac{1}{2})}{\Gamma(\frac{1}{4})} + \mathcal{O}\left(\frac{1}{L^{3/2}}\right). \quad (19)$$

Thus,  $\langle |m| \rangle L^{3/4}$  should approach  $0.909891\dots$  in the limit  $G \rightarrow 0$ . One indeed observes that the leftmost data points in the graph lie already very close to this limit. Together with the collapse of all numerical data onto a single curve, this also indicates that the simulations for systems with large interaction ranges indeed have been carried out at the correct temperatures; i.e., the extrapolation formula Eq. (14) has yielded sufficiently accurate estimates for the critical temperatures for  $18 \leq R_m^2 \leq 540$ . For the sake of clarity, it is stressed that for each single value of  $R$ , the simulations of the finite systems have been carried out at the critical temperature of a system with that particular interaction range in the thermodynamic limit.

As a side remark, I note that a much more sensitive description of the crossover can be formulated in terms of so-called “effective exponents”. Originally introduced by Kouvel and Fisher [32], they have found widespread use in experimental analyses (see, e.g., Ref. [24]) and more recently also in the analysis of numerical results, cf. Refs. [7,8,10,25]. Although these effective exponents are usually defined in terms of the logarithmic derivative with respect to the reduced temperature, an effective magnetic exponent can be introduced as

$$y_h^{\text{eff}} \equiv \frac{9}{4} + \frac{d \ln(\langle |m| \rangle L^{3/4})}{d \ln(L/R^4)}. \quad (20)$$

In the mean-field regime,  $y_h^{\text{eff}}$  does *not* approach the classical value  $y_h = 1 + d/2$ , but the corresponding value  $y_h^* = 3d/4$ . This is directly related to the violation of hyperscaling in the mean-field regime and can be explained from the dangerous-irrelevant-variable mechanism [33–35]. This is clearly illustrated in Fig. 8, where a smooth interpolation between the value  $9/4$  and the Ising value  $2.4815$  is found.

### C. Susceptibility

In a very similar way, the crossover function for the magnetic susceptibility  $\chi$  at criticality can be obtained. Since it is proportional to the average square magnetization density, it is independent of  $R$  in the mean-field regime. In the Ising regime, it scales as  $L^{2y_h-3}R^{2(9-4y_h)}$ , so that the quantity  $\chi L^{-3/2}$  can be represented as a function of the parameter  $G$ . Indeed, upon application of the range-dependent correction factor  $C[\chi]$ , which has the same form as the factor between brackets in Eq. (16), a perfect data collapse is obtained, see Fig. 9. The total crossover curve spans approximately four decades in  $G$ , just as for the magnetization density. The exact mean-field result expected here is  $\chi L^{-3/2} \rightarrow \sqrt{12}\Gamma(\frac{3}{4})/\Gamma(\frac{1}{4}) = 1.170\,829\dots$ , which is indeed well reproduced for the data in the regime  $G \rightarrow 0$ . No nonlinear finite-size effects can be observed, suggesting that these are (on the scale of the graph) negligibly small for  $L \geq 20$ .

### D. Fourth-order amplitude ratio

Rather than reproducing crossover curves for the connected susceptibility or the spin-spin correlation function, which are very similar to those presented in the previous two subsections, I prefer to pay some attention to the crossover of the amplitude ratio  $Q$ . This quantity, which is just a disguised form of the fourth-order cumulant introduced by Binder [36], attains trivial limiting values on either side of the critical temperature, but takes a nontrivial universal value at criticality. Its Ising limit  $Q_I = 0.6233$  (4) has already played an important rôle in Sec. III B, where this parameter was used to determine the location of the critical point. The critical value in the mean-field limit is known exactly,  $Q_{MF} = 0.456\,946\,58\dots$  [37,5]. Indeed, the full crossover from  $Q_{MF}$  to  $Q_I$  as a function of  $L/R^4$  can be observed, as illustrated in Fig. 10. No correction term has been applied here, because it may be expected that the correction terms for  $\langle m^2 \rangle^2$  and  $\langle m^4 \rangle$  cancel each other to a large extent, cf. Fig. 8 in Ref. [8]. The less smooth appearance of the crossover curve compared to that for the magnetization density and the susceptibility can mainly be attributed to several other effects. Apart from the much larger scale of the graph, it turns out that nonlinear finite-size effects are considerably stronger for  $Q$  than for other quantities. Further deviations are caused by imperfections in the estimates for  $T_c$  for large  $R$ , which on this scale become visible for the larger system sizes.

## VI. CONCLUSIONS

In this paper, I have presented a detailed determination of the critical properties of the three-dimensional equivalent-neighbor model, which is a generalization of the spin- $\frac{1}{2}$  Ising model, on a cubic lattice. Monte Carlo simulations have been carried out for systems with up to thirteen neighbor shells, corresponding to 250 equivalent neighbors. All systems have been shown to belong to the 3D Ising universality class. An analysis of these critical properties has yielded a coherent picture of their dependence on the interaction range  $R$ . The shift of the critical temperature as a function of interaction range, to which various mechanisms appear to contribute, has been determined and compared to theoretical predictions. I have shown that the range dependence of the critical finite-size amplitudes of the magnetization density and the magnetic susceptibility conform very well to the theoretically expected behavior. Also renormalization-group predictions for the variation of the finite-size corrections with interaction range have been confirmed and an estimate has been obtained for the effective interaction range at which the leading finite-size corrections should vanish. The numerical results support the expectation that the  $\phi^4$  coefficient in the Landau-Ginzburg-Wilson Hamiltonian varies monotonically with interaction range (or coordination number) and scales for large ranges as  $1/R^4$ . Further Monte Carlo results for systems with very large coordination numbers could be obtained by means of an efficient simulation scheme. These results enabled the mapping of the full finite-size crossover curves for several quantities, including the magnetic susceptibility and the fourth-order amplitude ratio. All these curves can be described by a single crossover parameter  $L/R^4$  and interpolate smoothly between mean-field and Ising-like behavior. Also the finite-size crossover function for the effective magnetic exponent  $y_h$  has been obtained.

A very interesting and experimentally most relevant extension of the work presented here is the case of *thermal* crossover, for which some first results have appeared in Ref. [10]. A more extensive analysis of this case will be presented elsewhere [9].

## ACKNOWLEDGMENTS

It is a pleasure to acknowledge stimulating discussions with Kurt Binder and Henk Blöte. I wish to thank Andrea Pelissetto for illuminating correspondence and John Rehr for sending me the series-expansion results of Ref. [28] and for permission to publish them. I thank the HLRZ Jülich for access to a Cray-T3E on which the computations have been performed.

---

- [1] C. Domb and N. W. Dalton, Proc. Phys. Soc. **89**, 859 (1966).
- [2] D. J. Thouless, Phys. Rev. **181**, 954 (1969).
- [3] K. K. Mon and K. Binder, Phys. Rev. E **48**, 2498 (1993).
- [4] E. Luijten, H. W. J. Blöte, and K. Binder, Phys. Rev. E **54**, 4626 (1996).
- [5] E. Luijten and H. W. J. Blöte, Int. J. Mod. Phys. C **6**, 359 (1995).
- [6] V. L. Ginzburg, Fiz. Tverd. Tela **2**, 2031 (1960) [Sov. Phys. Solid State **2**, 1824 (1960)].
- [7] E. Luijten, H. W. J. Blöte, and K. Binder, Phys. Rev. Lett. **79**, 561 (1997).
- [8] E. Luijten, H. W. J. Blöte, and K. Binder, Phys. Rev. E **56**, 6540 (1997).
- [9] E. Luijten and K. Binder, to be published.
- [10] E. Luijten and K. Binder, Phys. Rev. E **58**, R4060 (1998).
- [11] S. Caracciolo, M. S. Causo, A. Pelissetto, P. Rossi, and E. Vicari, preprint hep-lat/9809101.
- [12] R. Brout, Phys. Rev. **118**, 1009 (1960).
- [13] V. G. Vaks, A. I. Larkin, and S. A. Pikin, Zh. Eksp. Teor. Fiz. **51**, 361 (1966) [Sov. Phys.—JETP **24**, 240 (1967)].
- [14] N. W. Dalton and C. Domb, Proc. Phys. Soc. **89**, 873 (1966).
- [15] E. Luijten, *Interaction Range, Universality and the Upper Critical Dimension* (Delft University Press, Delft, 1997), Chap. 7.
- [16] K. Symanzik, Lett. Nuovo Cimento **8**, 771 (1973).
- [17] E. Brézin, J. C. Le Guillou, and J. Zinn-Justin, in *Phase Transitions and Critical Phenomena*, Vol. 6, edited by C. Domb and M. S. Green (Academic, London, 1976).
- [18] E. Riedel and F. Wegner, Z. Phys. **225**, 195 (1969).
- [19] M. E. Fisher, in *Critical Phenomena*, Proc. 51st Enrico Fermi Summer School, Varenna, Italy, edited by M. S. Green (Academic, N.Y., 1971).
- [20] J. Cardy, *Scaling and Renormalization in Statistical Physics* (Cambridge U.P., Cambridge, 1996).
- [21] H. W. J. Blöte, E. Luijten, and J. R. Heringa, J. Phys. A **28**, 6289 (1995).
- [22] A. J. Liu and M. E. Fisher, J. Stat. Phys. **58**, 431 (1990).
- [23] F. J. Wegner, Phys. Rev. B **5**, 4529 (1972).
- [24] M. A. Anisimov, A. A. Povodyrev, V. D. Kulikov, and J. V. Sengers, Phys. Rev. Lett. **75**, 3146 (1995).
- [25] M. A. Anisimov, E. Luijten, V. A. Agayan, J. V. Sengers, and K. Binder, preprint cond-mat/9810252.
- [26] H. W. J. Blöte, private communication.
- [27] M. Hasenbusch, K. Pinn, and S. Vinti, preprint hep-lat/9806012.
- [28] M. J. George and J. J. Rehr, “Critical properties of cubic Ising models”, unpublished.
- [29] A. J. Liu and M. E. Fisher, Physica A **156**, 35 (1989).
- [30] C. Domb, in *Phase Transitions and Critical Phenomena*, Vol. 3, edited by C. Domb and M. S. Green (Academic, London, 1974).
- [31] K. Binder and H.-P. Deutsch, Europhys. Lett. **18**, 667 (1992).
- [32] J. S. Kouvel and M. E. Fisher, Phys. Rev. **136**, A1626 (1964).
- [33] M. E. Fisher, in *Proceedings of the Summer School on Critical Phenomena, Stellenbosch, South Africa, 1982*, edited by F. J. W. Hahne (Springer, Berlin, 1983).
- [34] K. Binder, M. Nauenberg, V. Privman, and A.P. Young, Phys. Rev. B **31**, 1498 (1985).
- [35] E. Luijten and H.W.J. Blöte, Phys. Rev. Lett. **76**, 1557 (1996); **76**, 3662(E) (1996).
- [36] K. Binder, Z. Phys. B **43**, 119 (1981).
- [37] E. Brézin and J. Zinn-Justin, Nucl. Phys. B **257** [FS14], 867 (1985).
- [38] A. L. Talapov and H. W. J. Blöte, J. Phys. A **29**, 5727 (1996).

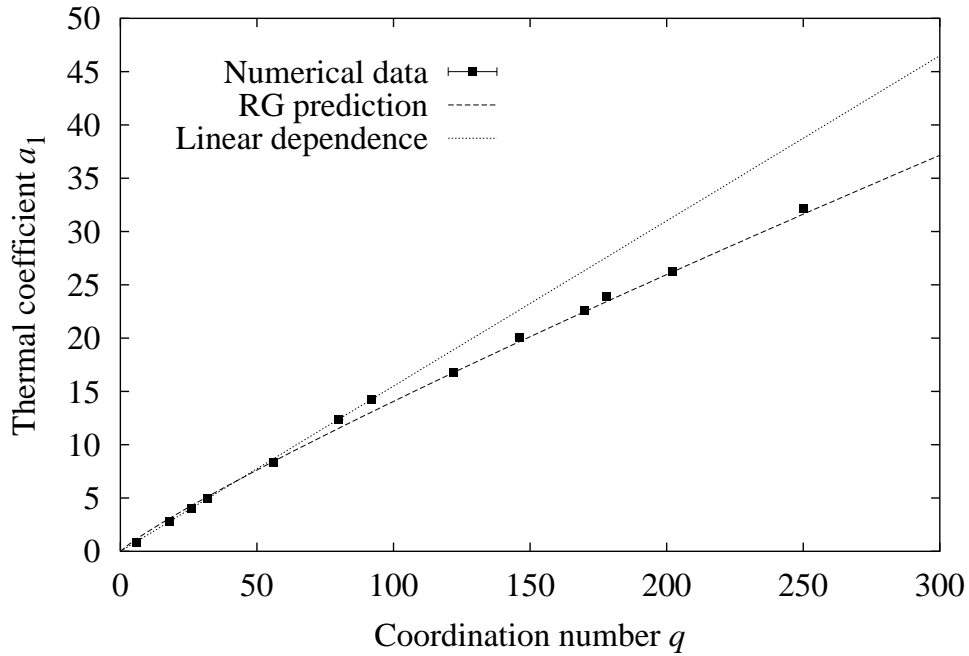


FIG. 1. The leading thermal coefficient in the finite-size expansion for the amplitude ratio  $Q$ , as a function of coordination number. The dashed curve shows the RG prediction (valid in the large- $q$  limit) of Ref. [4]. In order to appreciate the quality of this prediction, a linear  $q$  dependence is shown as well.

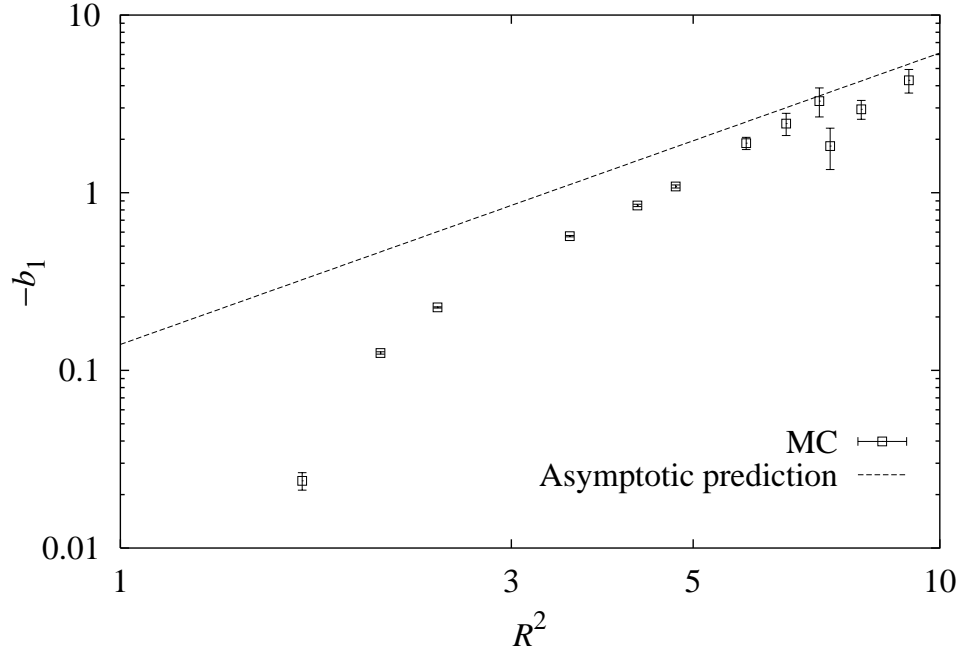


FIG. 2. Range dependence of the leading irrelevant field, cf. the second argument in the right-hand side of Eq. (4). Note that the result for  $R = 1$  is not shown, because it has the opposite sign. The dashed line represents the asymptotic expression,  $b_1 \propto R^{-4y_i/(4-d)}$ , as discussed in the text.

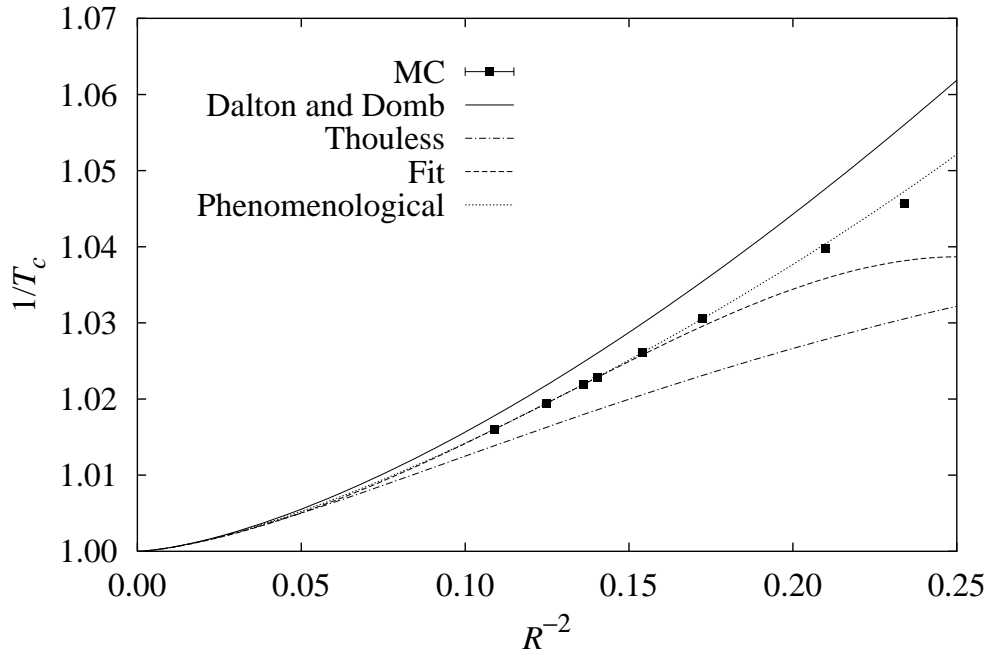


FIG. 3. Numerical results for the inverse critical temperature, normalized by the mean-field critical temperature, as a function of the inverse squared interaction range, together with the series-expansion results of Dalton and Domb [14] and Thouless [2]. The dashed and the dotted lines indicate the results of the least-squares fits discussed in Section IV A, where the dotted line is the phenomenological description in which lattice effects have been ignored.

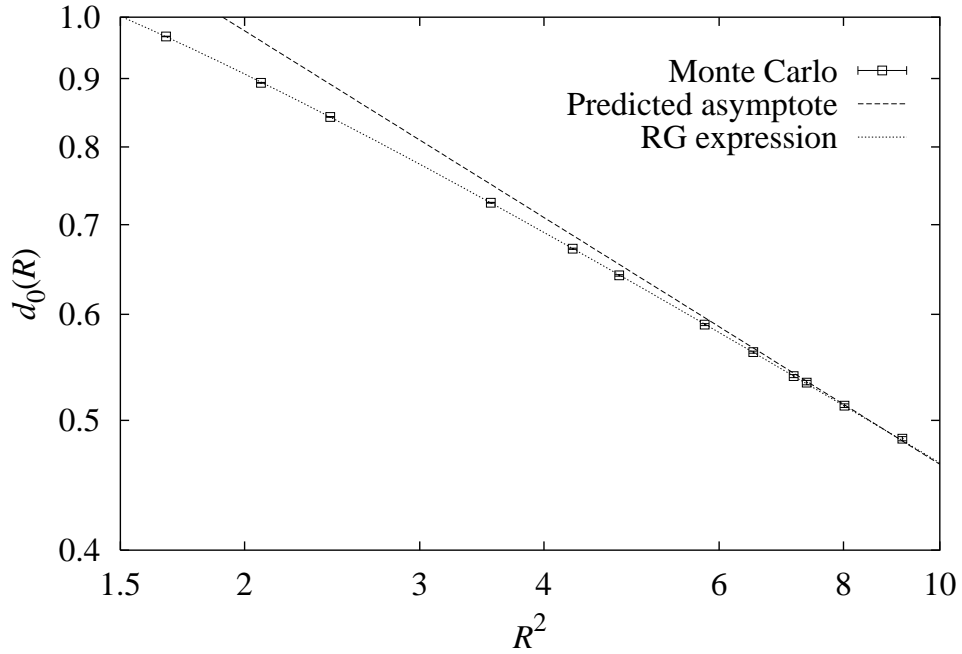


FIG. 4. Range dependence of the critical finite-size amplitude of the magnetization density, together with the predicted asymptotic range dependence (dashed line) and a fit of all the data points to the renormalization-group prediction (dotted curve).

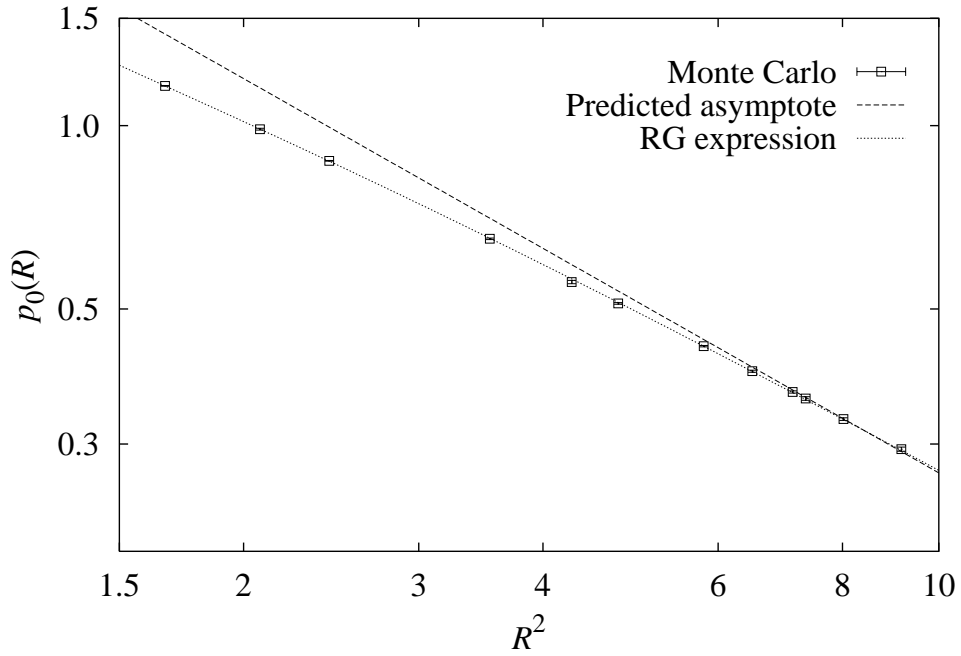


FIG. 5. Range dependence of the critical finite-size amplitude of the magnetic susceptibility, together with the predicted asymptotic range dependence (dashed line) and a fit of the data points to the renormalization-group prediction (dotted curve).

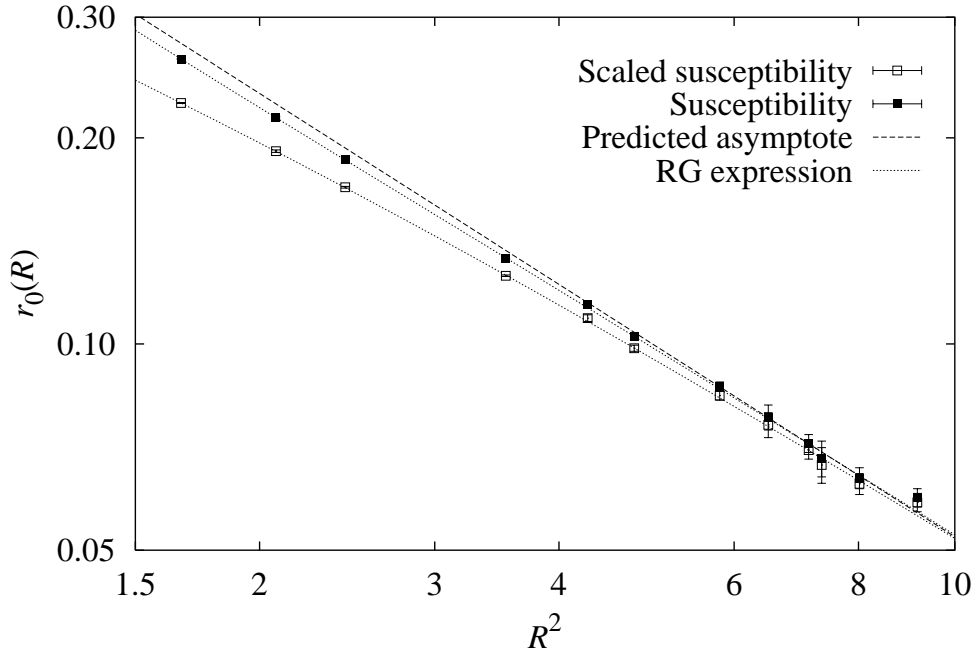


FIG. 6. Range dependence of the critical finite-size amplitude  $r_0(R)$  of the *connected* susceptibility, together with the predicted asymptotic range dependence and a fit of the data points to the renormalization-group prediction. Also the frequently-used *scaled* susceptibility is shown, which clearly exhibits stronger deviations from the asymptotic range dependence.

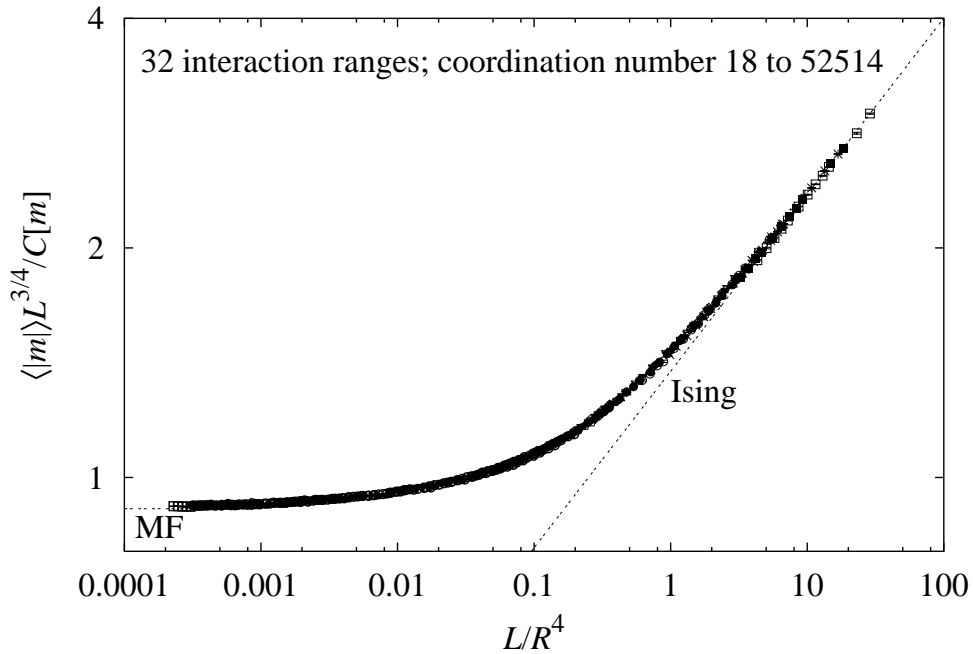


FIG. 7. Finite-size crossover curve for the absolute magnetization density  $\langle |m| \rangle$  multiplied by an appropriate power of the system size. For very small interaction ranges (rightmost data points), higher-order range dependences have been divided out, as indicated by the correction factor  $C[m]$  (for a more extensive discussion of this topic the reader is referred to the text). The crossover curve spans at least four decades in the parameter  $L/R^4$  and systems with a coordination number up to  $q = 52514$  had to be employed to fully reach the mean-field limit. The perfect collapse of all interaction ranges and system sizes confirms the validity of the crossover description in terms of a single parameter. The dashed lines denote the exact mean-field limit (“MF”) and the Ising asymptote with slope  $y_h = 9/4$ .

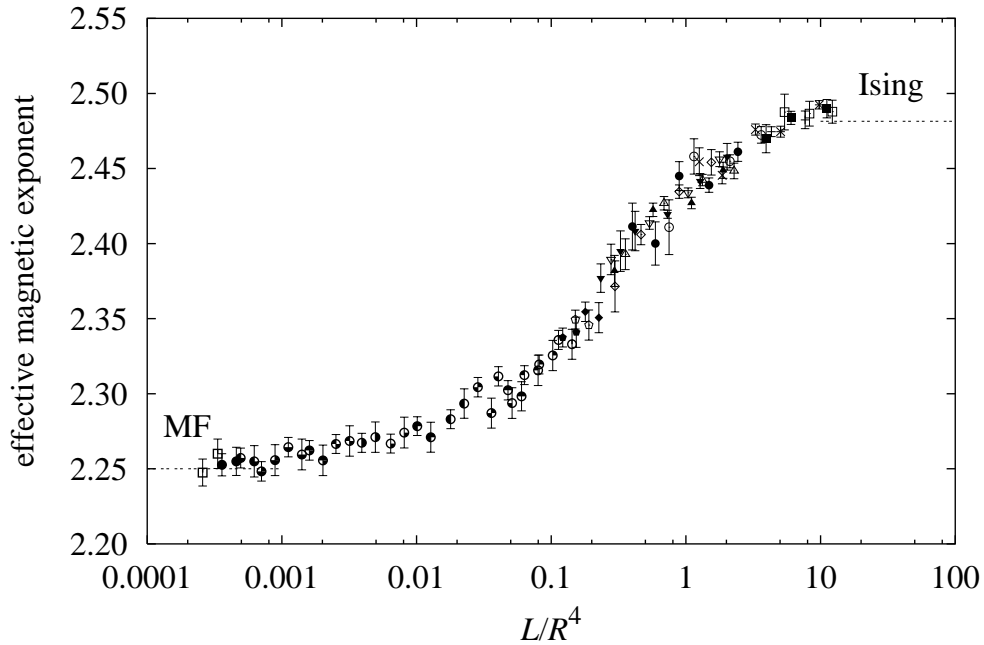


FIG. 8. The crossover behavior of the effective magnetic exponent as a function of the finite-size crossover parameter.

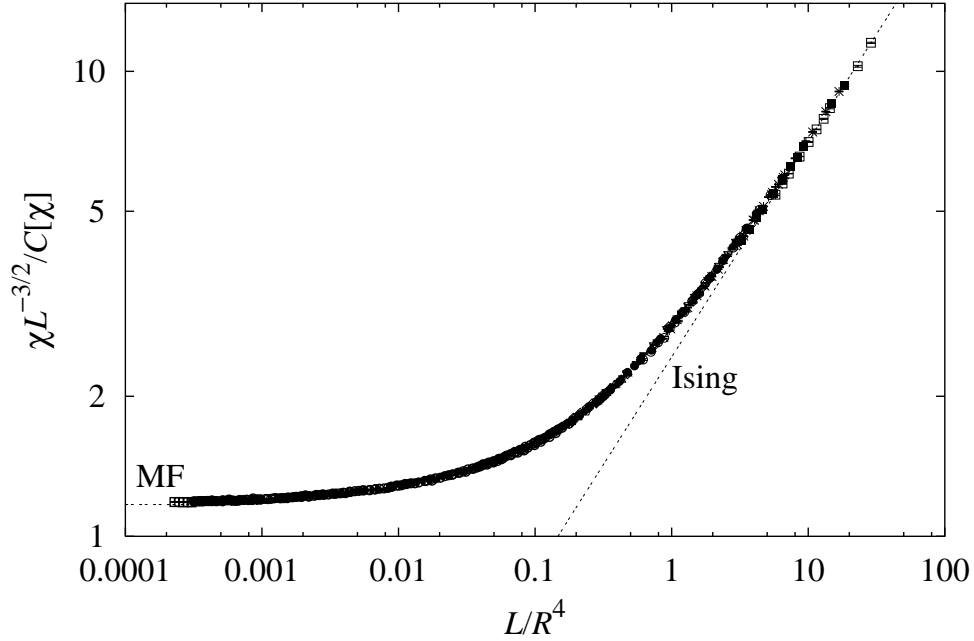


FIG. 9. Finite-size crossover curve for the magnetic susceptibility multiplied by an appropriate power of the system size. For very small interaction ranges (rightmost data points), higher-order range dependences have been divided out, as indicated by the correction factor  $C[\chi]$ . Just as in Fig. 7, systems with a coordination number up to  $q = 52514$  had to be employed to fully reach the mean-field limit. The perfect collapse of all interaction ranges and system sizes confirms the validity of the crossover description in terms of a single parameter. The dashed lines denote the exact mean-field limit (“MF”) and the Ising asymptote with slope  $2y_h - 9/2$ .

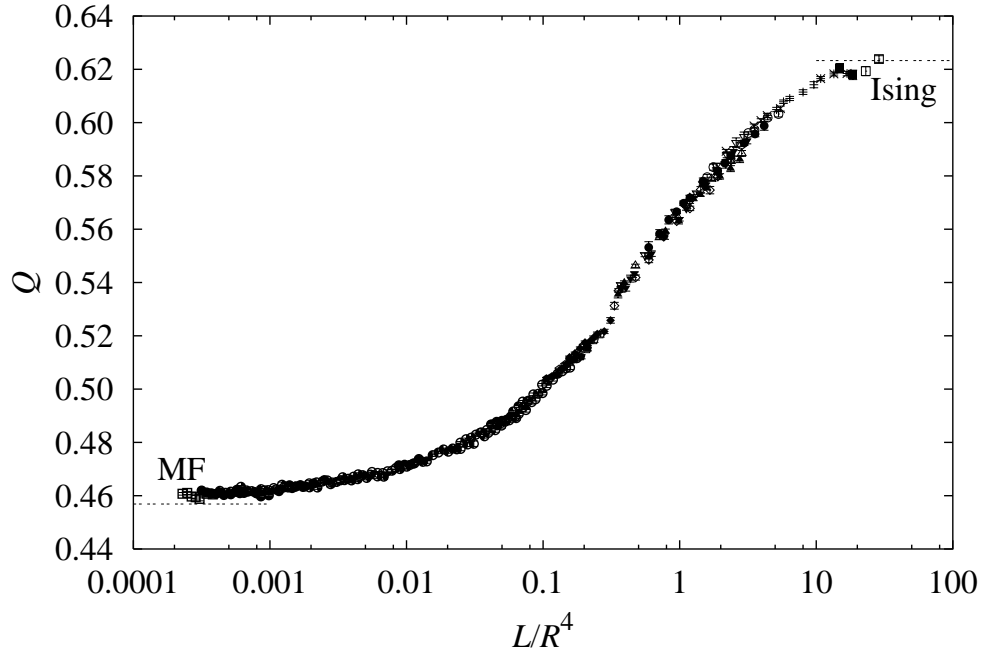


FIG. 10. Finite-size crossover curve for the amplitude ratio  $Q$ . It smoothly interpolates between the mean-field limit ( $L/R^4 \ll 1$ ) and the Ising limit ( $L/R^4 \gg 1$ ).



TABLE I. The range of interaction  $R_m$ , the corresponding number of neighbors  $q$ , and the effective range of interaction  $R$  for the thirteen neighbor shells examined in this work.

Shell	$R_m^2$	$q$	$R^2$
1	1	6	1
2	2	18	$\frac{5}{3}$
3	3	26	$\frac{27}{13}$
4	4	32	$\frac{39}{16}$
5	5	56	$\frac{99}{28}$
6	6	80	$\frac{171}{40}$
7	8	92	$\frac{219}{46}$
8	9	122	$\frac{354}{61}$
9	10	146	$\frac{474}{73}$
10	11	170	$\frac{606}{85}$
11	12	178	$\frac{654}{89}$
12	13	202	$\frac{810}{101}$
13	14	250	$\frac{1146}{125}$

TABLE II. The amplitude ratio  $Q$  and critical coupling  $K_c$  for the various ranges of interaction studied in this paper. The numbers in parentheses denote the errors in the last decimal places. The results for  $R_m^2 = 1$  (3D nearest-neighbor Ising model) stem from Ref. [21]. The fourth column shows the estimates for  $K_c$  obtained with  $Q$  fixed at the value found in the same work (the error margins include the uncertainty in  $Q$ ). For comparison, the estimates for  $K_c$  given in Ref. [1] are listed as well.

$R_m^2$	$Q$	$K_c$	$K_c$	$K_c$ [1]
1	0.6233 (4)	0.2216546 (10)		0.22171
2	0.6238 (8)	0.0644223 (5)	0.0644220 (5)	0.06450
3	0.6233 (8)	0.0430381 (4)	0.0430381 (4)	0.0432
4	0.6224 (5)	0.03432668 (12)	0.03432685 (15)	
5	0.6216 (14)	0.01892909 (7)	0.01892915 (4)	
6	0.621 (3)	0.01307105 (7)	0.01307111 (3)	
8	0.617 (4)	0.01130202 (8)	0.01130213 (3)	
9	0.608 (10)	0.00844691 (12)	0.00844703 (4)	
10	0.614 (11)	0.00702798 (9)	0.00702798 (4)	
11	0.61 (2)	0.00601661 (14)	0.00601663 (5)	
12	0.624 (11)	0.00574107 (7)	0.00574110 (4)	
13	0.618 (8)	0.00504666 (3)	0.00504666 (2)	
14	0.600 (14)	0.00406419 (4)	0.00406422 (2)	

TABLE III. The leading correction amplitudes appearing in the Wegner expansion for the magnetization ( $T < T_c$ ,  $a_m$ ), the magnetic susceptibility ( $T > T_c$ ,  $a_\chi$ ) and the squared correlation length ( $T > T_c$ ,  $a_{\xi^2}$ ), for three different lattice structures. The results for  $a_m$  were taken from Ref. [29] and the results for  $a_\chi$  and  $a_{\xi^2}$  from Ref. [28]. The (slight) nonmonotonicity as a function of coordination number in the latter two quantities, already noted in Ref. [22], is probably not significant and also appears to depend on the adopted choice for the susceptibility exponent  $\gamma$  (the present results correspond to  $\gamma = 1.237$ ). The results for  $a_m$  correspond to the somewhat too high value  $\beta = 0.3305$ , which can probably account for the difference with the result  $a_m \approx -0.203$  (for the sc lattice) obtained in Ref. [38].

	sc ( $q = 6$ )	bcc ( $q = 8$ )	fcc ( $q = 12$ )
$a_m$	-0.256	-0.240	-0.234
$a_\chi$	-0.108	-0.119	-0.114
$a_{\xi^2}$	-0.363	-0.217	-0.222

TABLE IV. The magnetic exponent  $y_h$  and the critical amplitude  $d_0(R)$  of the absolute magnetization density as a function of interaction range. The estimates for  $y_h$  in the third column have been obtained with  $K_c$  fixed at their best values given in Table II, whereas the critical amplitudes have been obtained with  $y_h$  fixed at its 3D Ising value.

$R_m^2$	$y_h$	$y_h$	$d_0(R)$
2	2.479 (2)	2.479 (1)	0.9674 (5)
3	2.479 (2)	2.481 (1)	0.8933 (6)
4	2.475 (5)	2.479 (1)	0.8424 (4)
5	2.477 (4)	2.480 (1)	0.7269 (5)
6	2.476 (6)	2.483 (2)	0.6716 (7)
8	2.472 (7)	2.484 (3)	0.6415 (9)
9	2.46 (2)	2.480 (3)	0.5895 (10)
10	2.47 (2)	2.478 (3)	0.5622 (10)
11	2.47 (2)	2.471 (5)	0.5395 (14)
12	2.53 (4)	2.485 (6)	0.5335 (20)
13	2.47 (2)	2.480 (5)	0.5128 (16)
14	2.463 (15)	2.475 (4)	0.4845 (17)

TABLE V. The magnetic exponent  $y_h$  and the critical amplitude  $p_0(R)$  of the magnetic susceptibility as a function of interaction range. The estimates for  $y_h$  in the third column have been obtained with  $K_c$  fixed at their best values given in Table II, whereas the critical amplitudes have been obtained with  $y_h$  fixed at its 3D Ising value. The data point for  $R_m^2 = 1$  is taken from Ref. [21].

$R_m^2$	$y_h$	$y_h$	$p_0(R)$
1			1.5580 (15)
2	2.479 (1)	2.479 (1)	1.1620 (7)
3	2.481 (6)	2.484 (3)	0.9865 (32)
4	2.478 (6)	2.484 (2)	0.8752 (12)
5	2.481 (8)	2.481 (3)	0.6518 (18)
6	2.478 (13)	2.478 (12)	0.5534 (35)
8	2.484 (14)	2.480 (2)	0.5105 (16)
9	2.46 (3)	2.476 (9)	0.4343 (12)
10	2.46 (2)	2.474 (4)	0.3951 (15)
11	2.46 (2)	2.47 (1)	0.3653 (16)
12	2.48 (2)	2.481 (6)	0.3564 (24)
13	2.46 (2)	2.484 (5)	0.3297 (16)
14	2.45 (4)	2.477 (6)	0.2943 (23)